https://doi.org/10.3311/PPci.41630

Periodica Polytechnica Civil Engineering

Determining the Actual Shape of a Bridge Pylon with Cylindrical and Conical Shapes Using Point Cloud Data and the RANSAC Shape Fitting Method

Shwana Manguri[1,2*], Bence Takács[1]

[1] Department of Geodesy and Surveying, Faculty of Civil Engineering, Budapest University of Technology and Economics, Műegyetem rkp. 3, H-1111 Budapest, Hungary
[2] Civil Engineering Department, University of Raparin, Ranya, Sulaymaniyah, Kurdistan Region, 46012, Iraq
[*] Corresponding author, e-mail: shwana.manguri@edu.bme.hu

Received: 16 July 2025, Accepted: 20 January 2026, Published online: 26 January 2026

Abstract

Determining the shape and deformations of structures with complex geometries has become an increasingly common task in the construction industry. This article presents a case study on determining the shape and deformation of a slope and circular steel structure, a cigar-shaped cable-stayed bridge pylon with varying cylindrical and conical shapes during three key construction stages using terrestrial laser scanning (TLS) point cloud data and the Random Sample Consensus (RANSAC) algorithm for shape fitting. A methodology involving vertical reorientation, point cloud slicing, and RANSAC-based circle fitting was applied to cross-sections of the pylon. Optimal RANSAC parameters were determined to be 80 iterations and a 5 mm tolerance, achieving reliable circle fitting with root mean square (RMS) errors predominantly within 3 mm across all scans. After initial steel frame installation, geometric distortion analysis revealed minimal deviations within a 2 mm radius error, a slight increase after concrete pouring, and a partial recovery in the final stage, except for a localized anomaly at the pylon's top. Deformation analysis along the pylon's axis showed maximum horizontal displacements of 65 mm according to the static models in the first scan, reaching a maximum of 269 mm after pouring concrete, with a subsequent reduction and change in direction after cable tensioning. This research demonstrates the efficacy of TLS and RANSAC for evaluating structural deformation and emphasizes the importance of parameter optimization for accurate point cloud analysis in complex civil engineering structures.

Keywords

complex structure, geometric distortion, pylon, RANSAC parameters, TLS

1 Introduction

In the last three decades, there has been a substantial increase in the desire to use advanced emerging technologies for inspecting, assessing, and managing civil infrastructure. Technologies like laser scanners have become compelling alternatives to traditional inspection and maintenance methods, which could be labor-intensive, costly, and unsafe. This trend is pronounced in the construction industry, typically in bridge monitoring [1, 2]. Terrestrial laser scanning (TLS) is a high-precision surveying technique that efficiently captures the spatial coordinates of objects of interest with incredible accuracy, remarkable precision at the millimeter level [2–5]. TLS employs multiple laser beams to hastily scan a target object, generating a dense point cloud that facilitates the construction of complex models. This technique gathers extensive 3D data over large areas, capturing a substantial number of laser measurements per second, optimizing performance efficiency [2, 6]. The key advantage of TLS is its non-contact operation, eliminating potential harm or interference that traditional measurement methods may cause [1, 7]. Furthermore, TLS is adversely affected by external environmental factors, ensuring stability in challenging conditions characterized by multiple light sources or intense lighting, complex backgrounds [8]. Its full-range scanning capabilities enable data capture of both horizontal and vertical planes, providing extensive information for deformation monitoring, panoramic photograph views, and incoming light intensity of the target object. Given its extreme precision, high data density, efficiency, non-contact measurement approach, and reduced susceptibility to

Cite this article as: Manguri, S., Takács, B. "Determining the Actual Shape of a Bridge Pylon with Cylindrical and Conical Shapes Using Point Cloud Data and the RANSAC Shape Fitting Method", Periodica Polytechnica Civil Engineering, 2026. https://doi.org/10.3311/PPci.41630

external interference, TLS has become an indispensable tool for deformation monitoring, with widespread applications across various industries [9, 10]. While TLS is utilized for deformation monitoring, defining the scanning area based on the shape and size of the object is crucial to ensure measurement accuracy [11]. Nevertheless, many factors may impact the accuracy of laser scanner observations, including laser power, ambient lighting conditions, and scanning speed [12].

Structural deformation analysis with point cloud shape fitting using the Random Sample Consensus (RANSAC) algorithm includes detecting and quantifying changes in a structure's geometry over time by fitting geometrical shapes like planes and cylinders to point cloud data. Then, RANSAC is used in subsequent scans to refit the model to updated point clouds. Deviations between the initial model and the new fits are calculated to detect structural deformations, like shifts in alignment, radius changes, or tilt [1].

Fischler and Bolles [13] introduced the Random Sample Consensus RANSAC algorithm, a widely employed robust estimator designed to fit models to datasets containing a significant proportion of outliers. Operating under a hypothesize-and-verify framework, RANSAC iteratively selects minimal random subsets of data points to hypothesize model parameters. Each hypothesized model is then evaluated against the entire dataset to determine its support and the number of data points consistent with the model within a predefined threshold [14–16].

A key strength of RANSAC lies in its tolerance to a significant fraction of outliers, making it an important tool in various fields. In computer vision, it is used for tasks such as estimating epipolar geometry, homographies, and fundamental matrices. RANSAC has also been successfully applied in image registration, including the automated registration of satellite images. Furthermore, in geodesy and LiDAR data processing, it is utilized for point cloud segmentation and registration, as well as for fitting geometric primitives like planes and spheres to point clouds [17–22]. The performance of RANSAC is affected by multiple input parameters, including the minimum number of points required to define the model, the expected percentage of inliers, the desired probability of finding a good model, and the threshold value for determining inliers. The algorithm repeats the postulate and verification process until a termination criterion, based on the desired confidence level, is met. Owing to its stochasticity, the results of RANSAC can change over multiple runs on the same data, highlighting the importance of evaluating its reliability. Several modifications and improvements to the basic RANSAC algorithm have been recommended to enhance its efficiency and robustness for particular applications [14–16, 23].

This paper investigates the deformation behavior of a pylon by analyzing geometric distortions and potential rotations around its central axis throughout different stages of construction. Beyond the deformation analysis, the study also aims to evaluate the robustness and reliability of RANSAC-based algorithms for geometric feature extraction from point cloud data. This research promotes understanding of deformation monitoring and using point cloud processing strategies in structural assessments by addressing structural performance and computational accuracy.

2 Methodology

The precise measurement and analysis of the geometry of complex structures, such as sloped cylindrical and conical pylons (e.g., the pylon of cable-stayed bridges), pose significant challenges in engineering surveying. Conventional instruments, such as total stations, depend on clearly defined markers for accurate measurements; however, these reference points are often absent on smoothly varying surfaces. Additionally, the direct manipulation and analysis of these structures in three dimensions is inherently complex due to the complexity of reconstructing their exact geometry from discrete measurement data. A robust methodological framework is utilized to tackle these challenges, which leverages point cloud data for structured analysis. This method consists of slicing the point cloud into a series of cross-sections along the longitudinal axis of the pylon, thus turning a 3D problem into a series of 2D problems. Each cross-section is examined, and the contour points are extracted and fitted to an assumed ideal circular cross-section as shown in Fig. 1. The actual axis of

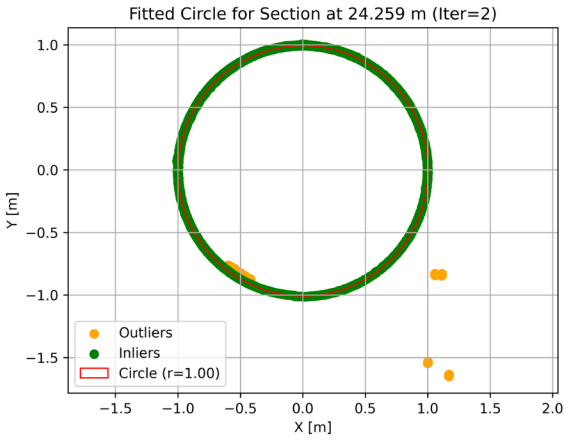

Fig. 1 Fitted circle along axis 24.259 m of scan 3 measured data

the pylon is derived from the center points of the circles, enabling a direct comparison between the designed geometries and the as-built. This workflow transforms a complex 3D reconstruction object into a more manageable and precise analysis, ensuring accurate evaluation of geometric deviations for quality control and structural assessment.

Since the pylon has a slope, obtaining consistent cross-sections from direct analysis of the object in its original orientation for geometry assessment is difficult. Thus, a transformation is applied to reposition the pylon into a vertical orientation to measure the pylon correctly. The transformation permits cross-sections of the structure to be drawn perpendicular to the re-aligned longitudinal axis instead of slicing across oblique plane. As a result, these cross-sections consistently reflect the structure's actual geometry at different heights. The transformation refines contour point extraction accuracy and circular fits/axis reconstruction, free from the effects of the original slope.

A RANSAC algorithm is a distinct option that should be applied to lines, planes, and spheres to determine the geometry of measured shapes accurately. RANSAC is highly beneficial because it can handle noise and outliers, ensuring reliable model fitting even in the presence of measurement errors or local irregularities. The RANSAC algorithm is commonly employed due to its robustness [13, 24, 25]. The RANSAC procedure involves randomly selecting a set of data points necessary to define a model, referred to as parameter estimation. These points are used to establish the model and calculate the deviation of all other data points from it [26]. Data points are classified as outliers and inliers based on their distance to the model. Points that fit the model within a defined tolerance are inliers, while those that do not are outliers. Each iteration selects a new random set of data points to define the model, and the count of inliers is determined. This process repeats for a specified number of iterations, and the solution with the highest number of inlier points is chosen. For this solution, the best-fitting model is refined using a method like least squares.

Advances in computational power allow for hundreds or thousands of iterations. However, the method is non-deterministic, meaning it provides a correct result only with a certain probability, which can be improved by increasing the number of iterations. Another drawback is its sensitivity to parameter selection (tolerance, iteration count), as these parameters are highly dependent on the dataset [1, 25]. The required number of iterations can be estimated using the Eq. (1) follows the formulation presented in [23]:

$$k = \frac{\log\left(1-p\right)}{\log\left(1-w^{n}\right)}, \tag{1}$$

where: k is the number of iterations, n is the lowest number of points to uniquely define the model, p is the desired probability (confidence level) that RANSAC selects at least one sample consisting entirely of conformal (inlier) points belonging to the fitted circle, typically set to 0.99, and w is the proportion of occurrence of conformal data.

RANSAC can detect particular shapes in a point cloud, such as planes, spheres, cylinders, and cones, with only up to 50% of the points not adhering to the model. RANSAC is employed to fit 2D shapes such as circles by making repeated random samples of a minimal subset of points to fit the best model. Specifically, three points are randomly selected for circles at a time used to define the candidate circle. The remaining points are evaluated to determine how well they conform to the model using a pre-determined threshold value. Points within the threshold regarding distance to the candidate circle are deemed inliers, while points further from the candidate geometry are outliers. RANSAC applies this method to perform groups of random selections to converge upon a model that maximizes the number of inliers and generally yields the fitted circle that is most robust to noise or outlier points.

Configuring RANSAC parameter settings, including the iteration count and the tolerance threshold is essential for attaining precise geometric fitting in point clouds; refer to Fig. 2, a flowchart of the RANSAC parameter setting up. A deficient number of iterations may not discern the appropriate model, whilst excessive iterations elevate computing expenses without substantial improvements in accuracy. The parameter tolerance threshold must balance the noise resistance and the incorporation of valid inliers. The parametrization of the algorithm is optimal, which requires iterative fine-tuning of parameters and some prior knowledge regarding the constraints of the dataset to balance accuracy and efficiency. This iterative improvement improves the robustness of the estimates of the model through consideration of measurement noise and structural irregularities. This repetitive refinement enhances the reliability of the estimated model by allowing variations in measurement noise and structural irregularities. The fitting quality is evaluated through root mean square (RMS) error calculations, which quantify the accuracy of the identified circles. Furthermore, the ratio between outliers and inliers and the number of outlier and inlier points is computed. The detected x and y coordinates

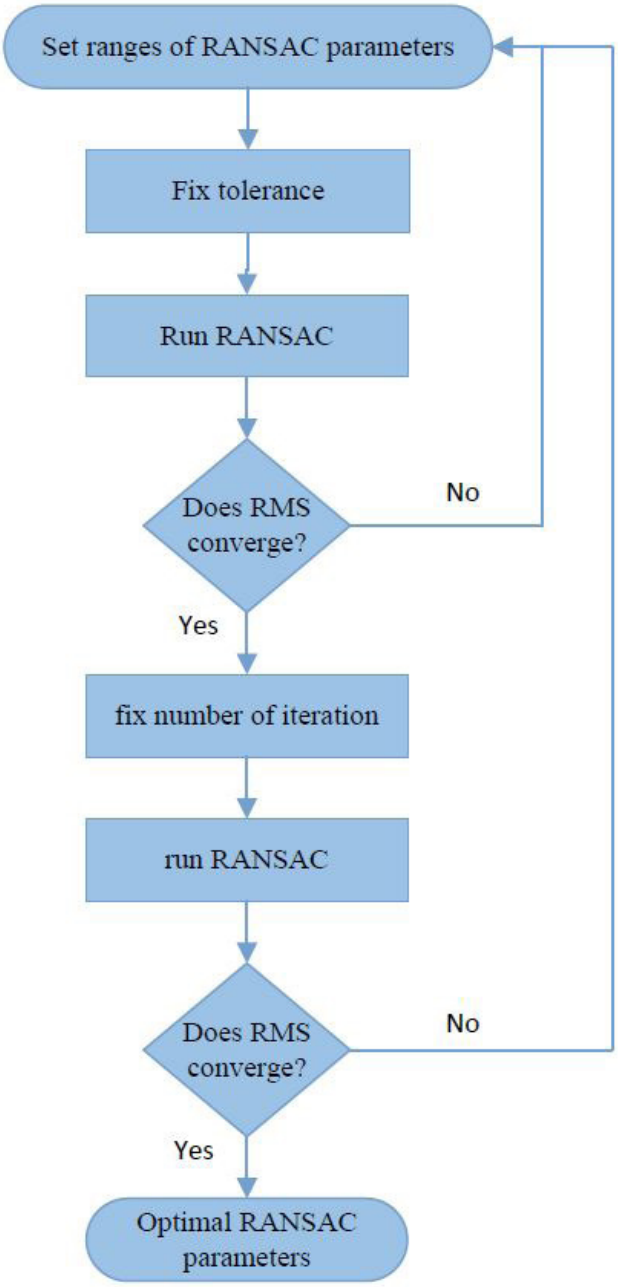

Fig. 2 Flowchart of RANSAC parameter setting up

of the circles and their corresponding radius are thus extracted as geometric parameters, which describe the circular features in a detailed way. Upon reviewing the literature, we found a lack of studies addressing the issue of selecting appropriate RANSAC parameters to obtain reliable results. Ref. [23] is among the limited studies explicitly examining parameter selection of the RANSAC algorithm and its impact on geometric shape detection in point clouds. The inlier percentage and threshold variation effects on plane and sphere modeling from laser scans were analyzed through simulation. Outcomes underline the efficiency of RANSAC; however, they highlight the need for several repetitions and preceding knowledge for reliability. Additionally, [16] examines the reliability of the RANSAC algorithm in estimating geometric parameters in point cloud data, which is commonly used in geodetic surveying. Whereas RANSAC effectively detects shapes such as planes, spheres, and cones, its consistency is frequently overlooked. These authors assess reliability by repeatedly applying RANSAC over the same dataset and analyzing parameter variation across runs rather than relying only on inlier residuals. Results indicate that a single RANSAC run may overestimate accuracy, emphasizing the need for multiple repetitions to enhance reliability.

Equation (1) recommends 34, 70, 168, 573, 4603, and 36839 iterations for fitting a circle to points in a point cloud with (n = 3) and an assumed 50%, 40%, 30%, 20%, 10%, and 5% inlier ratio, respectively. The tolerance value, crucial to the fitting process, should be determined by the user based on experience and preliminary calculations. The tolerance selection and the model's accuracy assessment can be informed by examining the fit residuals and the precision of the model parameters established during adjustment.

The optimized RANSAC parameters were determined through a comprehensive parameter study, involving various repetition levels, a high number of iterations, and systematically varied tolerance thresholds for each configuration. The pylon structure was segmented into predefined sections at constant intervals and RANSAC was applied to assess convergence behavior. Across the entire dataset, several million circles were generated.

3 Data acquisition from the Robinson Bridge

The Robinson Bridge, a pedestrian and cycling bridge between South Pest and Csepel in Budapest, spans the mouth of the Danube branch in Ráckeve. It connects the National Athletics Stadium with its training fields. Officially named the pedestrian bridge on Split Island (Osztósziget), it is also referred to as Robinson Bridge, as the island is known as Robinson Island. This 168-meter cable-stayed bridge features concrete-lined steel tubes and an orthotropic deck. The 64-meter-high steel pylon on the island is anchored by 53 inclined cables and three back cables, supporting the 7-meter-wide deck. With a unique design, the steel structure has no intermediate fixed supports. The bridge was designed by Speciálterv Ltd., with Gábor Pál as the lead designer [26], the pylon's profile varies along the center line as shown in Fig. 3.

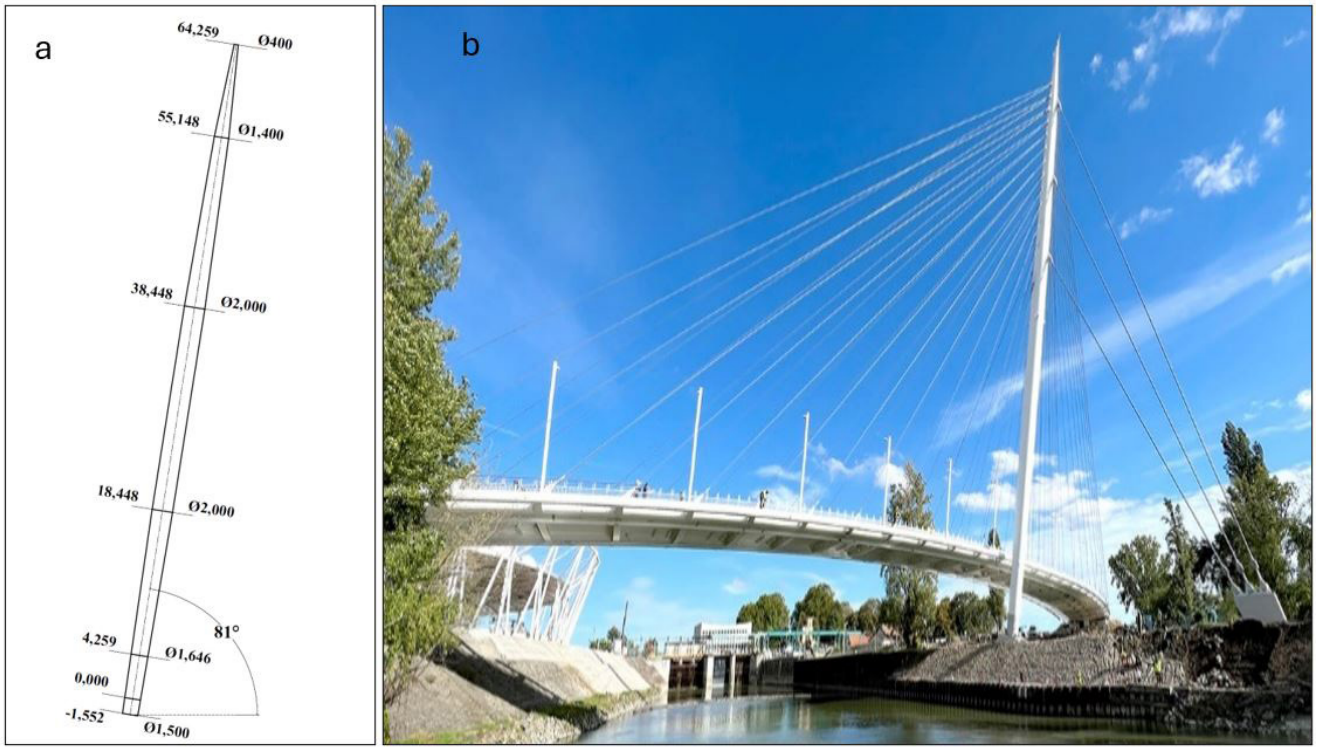

Fig. 3 (a) The Robinson Bridge pylon profile, (b) The Robinson Bridge

During the data collection phase, we measured the shape of the pylon at three key construction stages and compared these measurements to the shape derived from structural models. The first measurement phase occurred on January 17, 2022, after the steel-framed pylon was installed, resulting in the collection of 3.9 million points at a surrounding temperature of 3 °C. The second phase occurred on June 9, 2022, following the completion of the pylon's concrete structure, during which 2.5 million points were collected at 20 °C. The final measurement was conducted on August 30, 2022, after the cables were tensioned and the temporary supports and track structure were removed, yielding 15.8 million points at 20 °C. Scans 1, 2, and 3 will represent the first, second, and third measurements.

The measurements were carried out using a Leica C10 terrestrial laser scanner. Point clouds from multiple scanning positions were registered with each other using reference markers and aligned with the construction network system. The coordinates of these reference points were determined using a robotic total station, achieving registration and alignment within a few millimeters of accuracy.

4 Results

4.1 RANSAC parameters assessment for circle fittings

This study uses RANSAC as a robust method for detecting circular features in 3D point cloud data. Spatial data is transformed to make the aforementioned algorithm simpler to apply. The transformation parameters are derived from the pylon plan, involving a translation and a rotation around the z-axis and x-axis.

The point cloud was intersected every 1 meter along the axes of the pylon with a section thickness of 5 cm. This thickness was chosen to balance structural detail preservation and computational efficiency. It ensures sufficient geometric information for accurate feature extraction while minimizing excessive noise and overlap. A thinner section might lack data for reliable fitting, whereas a thicker one could introduce unnecessary complexity. This thickness aligns with typical engineering tolerances, reduces sensitivity to minor point cloud irregularities, and maintains consistency with the precision of terrestrial laser scanning, ensuring stable and meaningful geometric analysis. The section points were then used for circle fitting through an iterative robust estimation process employing the RANSAC procedure.

The parameters were set accordingly to evaluate the RANSAC method. It has executed 1, 5, and 10 repetitions to achieve this, with iterations ranging from 1 to 100 and a systematically varying tolerance ranging from 1 mm to 20 mm in increments of 1 mm. The pylon was divided into 60 sections to analyze convergence behavior. For the whole data set, 1.2 million circles were

generated. Inaugural, to increase the likelihood of finding an optimal model, we set the number of repetitions to 10 as an initial stage of parameter configuration. Establishing clear convergence criteria is crucial for ensuring the reliability of the estimated parameters. First, the scatter plots of all three scans in Fig. 4 illustrate the root mean square (RMS) values in millimeters as a function of the number of iterations for all evaluated sections while the tolerance is fixed. Each blue dot represents the RMS error for a circle fitted at a given iteration step. Initially, the data exhibits high fluctuation and multiple outliers, particularly within the first 20 iterations, where RMS values occasionally exceed 200 mm. However, as the number of iterations increases, the RMS values sharply fall and stabilize. Approximately 80 iterations, the RMS values consistently converge toward a low range, indicating minimal error and improved fitting accuracy. This convergence behavior confirms that 80 iterations are sufficient to generate circles reliably with confident RMS values, ensuring accurate section-fitting results across the dataset.

Fig. 5 illustrates the relationship between the RMS and tolerance when the number of iterations is fixed at 80. The scatter plot shows a relatively consistent RMS distribution across the full range of tolerance values from approximately 1 mm to 20 mm. The lack of a clear rising or falling trend suggests that variations in tolerance have little to no significant effect on the RMS. Based on this observation, a tolerance value of 5 mm is selected as a reasonable and stable parameter for subsequent analysis. At this stage RMS stabled between 2 to 3 mm.

The fixed tolerance of 5 mm and 80 iterations for three measurement stages Scan 1, Scan 2, and Scan 3 was

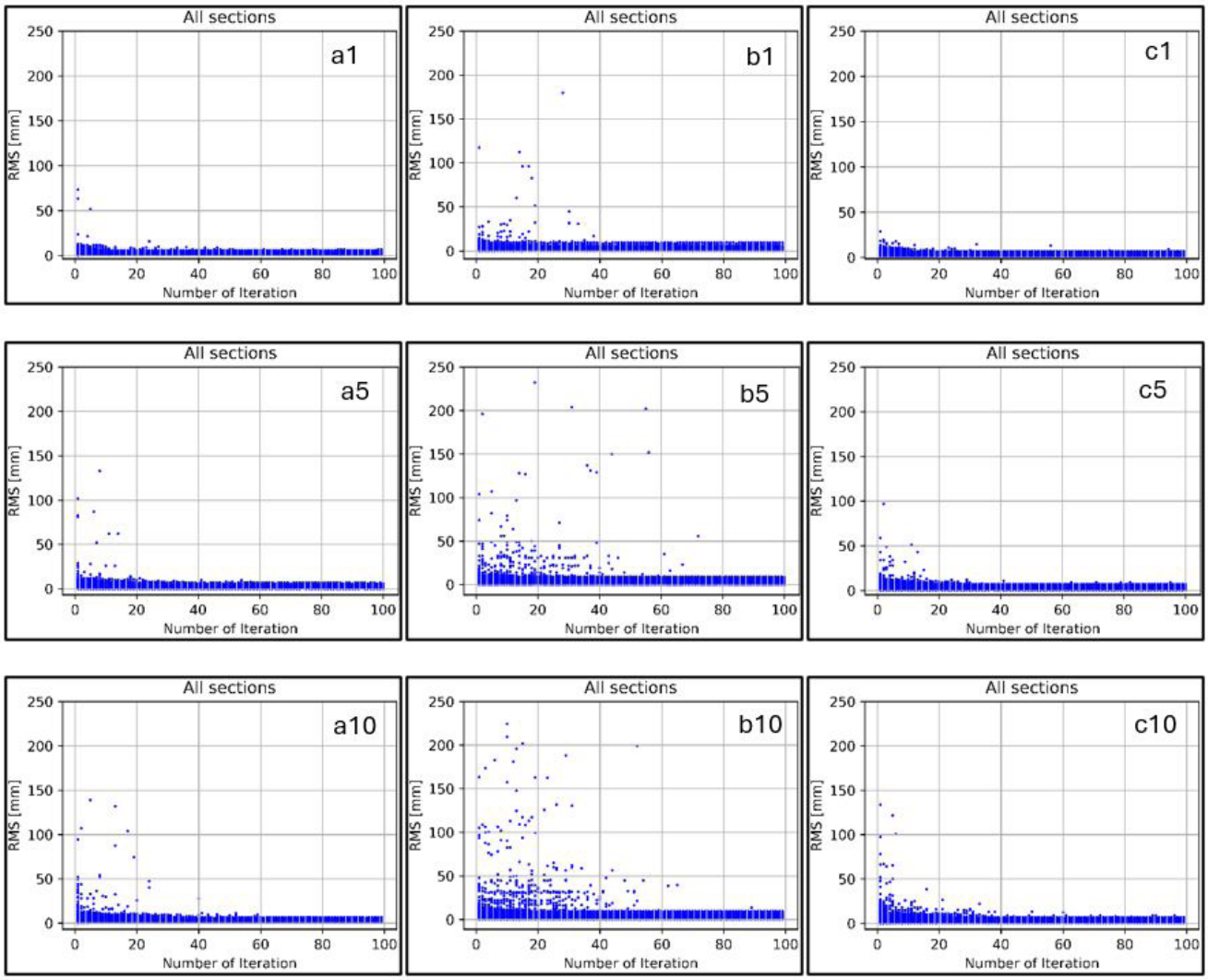

Fig. 4 Iteration of all sections versus RMS (a1, a5, a10) Scan 1, (b1, b5, b10) Scan 2, and (c1, c5, c10) Scan 3, while values 1, 5, and 10 represent the number of repetitions

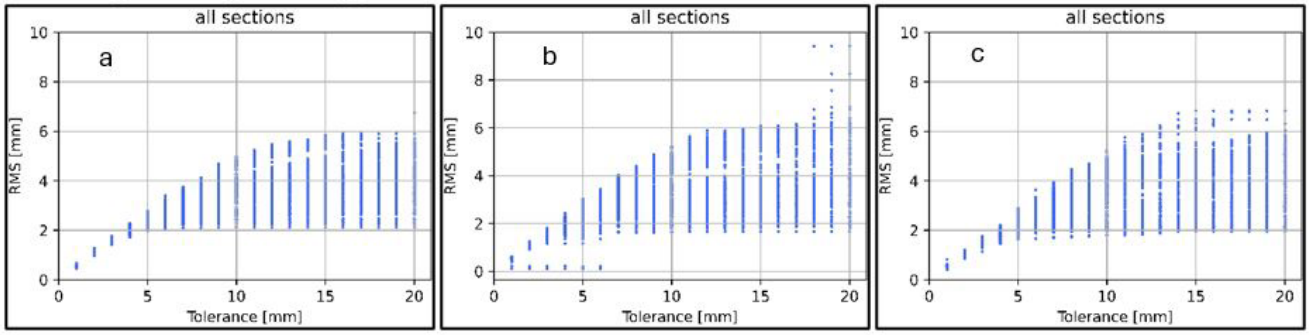

Fig. 5 Tolerance for iteration 80 of all sections versus RMS (a) Scan 1, (b) Scan 2, and (c) Scan 3

conducted, illustrating the RANSAC fitting performance. The RMS error is presented for each scan, reflecting the fitting accuracy across individual sections. The results explore that the RMS values persist at consistently low levels, predominantly within the 1–3 mm range across all scans. Although Scan 2 exhibits slightly more significant variation, the overall differences are minimal, indicating that the employed parameters yield reliable and accurate circle fitting for each measurement phase.

The error in the estimated radius is calculated as the difference between the planned (design) radii and those obtained from fitted circles at each section across all three measurement phases presented in Table 1. This comparative assessment was performed to evaluate the reliability and stability of the circle fitting process using RANSAC with multiple iterations. The deviation in radius converged along the iterations until it reached around 80 iterations. Then, the deviation in radius remained consistently low for most sections in all scans around 3 mm, indicating a minimal discrepancy between the planned and fitted geometries. This consistency supports the outcome that using 80 iterations is sufficient to achieve accurate and reliable circle fitting, as confirmed by the low RMS values. The results prove the robustness of the fitting process under the specified conditions and validate the methodological choice.

According to the analysis, 80 iterations are recommended for reliable circle fitting, corresponding to an inlier ratio of approximately 37%. During the RANSAC-based fitting process, a threshold of 5 mm proves sufficient for achieving accurate results. While increasing the number of repetitions plays a critical role in increasing the likelihood of finding an optimal model, we set the number of repetitions to 10. The proposed approach demonstrates high robustness in detecting circular structures within complex 3D environments. The combination of spatial transformation, sectioning, and iterative model refinement ensures reliable feature extraction, even in significant noise.

Table 1 Error in the estimated radius along three phases of the construction

Elevation (m)	Planned radius (mm)	Scan 1		Scan 2		Scan 3	
		Measured radius (mm)	Radius error (mm)	Measured radius (mm)	Radius error (mm)	Measured radius (mm)	Radius error (mm)
4.259	823	824	−1	817	+6	828	+5
9.259	885	887	−2	887	−2	886	+1
14.259	948	950	−2	950	−2	949	+1
19.259	1000	1001	−1	1001	−1	1000	0
24.259	1000	999	+1	1000	0	999	−1
29.259	1000	1000	0	1000	0	999	−1
34.259	1000	1001	−1	1000	0	999	−1
39.259	985	986	−1	984	+1	984	−1
44.259	896	896	0	894	+2	894	−2
49.259	806	807	−1	804	+2	805	−1
54.259	716	717	−1	715	+1	716	0
59.259	474	473	+1	470	+4	473	−1
64.259	200	200	0	---	---	---	---

4.2 Robinson Bridge pylon deformation monitoring

The centers of the fitted circles reveal the actual shape of the pylon's axis. The ideal axis shape is represented by a straight line, making an angle of 81° with the horizontal and 251.95206° with the north according to the plans. However, the pylon's structure is deformed, deviating from the ideal shape due to its self-weight, temperature variations, environmental influences (e.g., wind), and the track structure suspended through the cables, which serves as a load. The deformations were calculated using static models based on the finite element method. The designer provided the calculated deformations at specific points, as listed in Table 1, measured at 5-meter intervals along the pylon's axis.

According to the design specifications, the actual deformations at these points were to be determined and compared to the calculated values. The designer also set tolerances for the deviation between the actual and estimated values, expressed as a fraction of the distance measured along the pylon axis.

The deformations of the pylon measured at three different times during data collection are presented in the direction of the pylon's tilt, as Yc, and perpendicular to it, as Xc, relative to the ideal shape in Fig. 3(a). In the direction of the tilt, positive deformation indicates a shift toward the track structure, while in the perpendicular direction, positive deformation indicates a shift toward Csepel Island, which refers to a horizontal displacement approximately in the northeast–southwest direction that is perpendicular to the pylon's tilt direction (251.95206°). Fig. 6 shows that in Scan 1, the maximum deformation of the steel structure due to self-weight was −65 mm in the direction of tilt and +45 mm perpendicular to it. In Scan 2, deformations increased after the steel structure was concreted, with a maximum value of −269 mm in the tilt direction and +55 mm perpendicular to it. In Scan 3, after the suspension of the track structure, tensioning of the cables, and removal of the temporary supports for the pylon and track structure, the direction of the deformations changed, and their magnitude decreased slightly compared to the Scan 2 measurements.

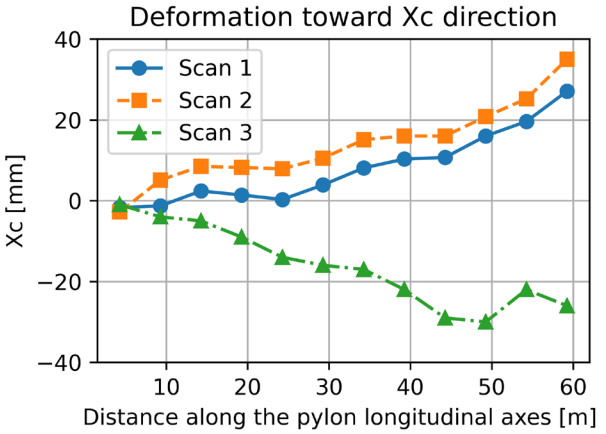

(a)

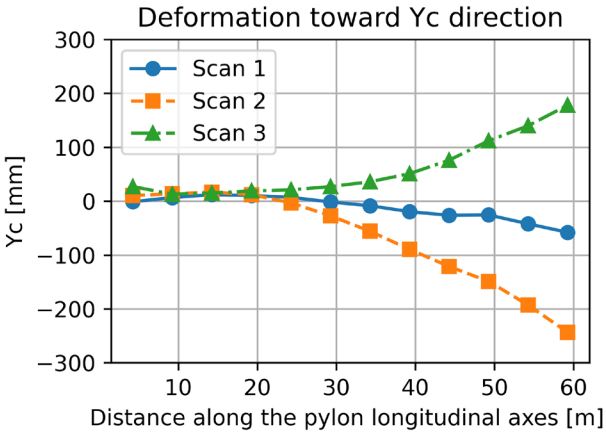

(b)

Fig. 6 Deformation of the pylon toward (a) the Xc and (b) Yc directions

5 Conclusions

Accurately assessing the shape and deformation of geometrically complex structures is becoming increasingly necessary in the construction sector. This paper details a case study that characterizes the shape and deformation of a roughly 65-meter-long, circular steel structure featuring a variable radius. A significant challenge arose from the absence of readily measurable points using conventional geodetic techniques, necessitating data acquisition via terrestrial laser scanning from multiple viewpoints.

Our developed methodology addressed this challenge by intersecting the acquired point cloud data with planes oriented perpendicularly to the planned axis of the pylon. Subsequently, circles were fitted to the point distributions within these cross-sections using an iterative and robust Random Sample Consensus (RANSAC) procedure. Despite a substantial proportion of outlier points (approximately 20-60%) within each intersection, the center and radius of the fitted circles were determined with millimeter-level accuracy. The deformations measured using the proposed approach strongly supported those predicted by static structural models, confirming that the structure's response to applied loads aligned with anticipated behavior.

This research successfully determined the actual shape of the Robinson Bridge pylon at three distinct construction phases by employing TLS point cloud data and the RANSAC shape fitting method. The methodology, which

included data transformation, point cloud slicing, and iterative circle fitting, proved effective in analyzing the pylon's geometry and deformation. The assessment of RANSAC parameters revealed that 80 iterations and a tolerance of 5 mm yielded reliable and consistent circle fitting results across all measurement stages with consistently low RMS errors (0–3 mm). While increasing the number of repetitions initially improved the stability of the inlier percentage, it did not significantly enhance the final fitting quality beyond a certain point, suggesting an optimal balance between accuracy and computational efficiency.

The analysis of geometric distortions revealed that the pylon experienced the most significant changes after concrete pouring. Subsequent cable tensioning led to a partial recovery of the intended geometry. Furthermore, the horizontal deformation analysis along the pylon's axis indicated substantial displacements, reaching a maximum of −269 mm in tilt direction after completion of the concrete work. These deformations partially recovered and shifted direction after the cables were tensioned. The findings underscore the efficacy of the presented methodology for detailed deformation monitoring of complex bridge pylons using point cloud data and robust fitting techniques. The study also emphasizes the necessity of careful RANSAC parameter selection to achieve accurate and dependable results in real-world structural assessments.

References

[1] Shen, N., Wang, B., Ma, H., Zhao, X., Zhou, Y., Zhang, Z., Xu, J. "A review of terrestrial laser scanning (TLS)-based technologies for deformation monitoring in engineering", Measurement, 223, 113684, 2023. https://doi.org/10.1016/j.measurement.2023.113684

[2] Rashidi, M., Mohammadi, M., Kivi, S. S., Abdolvand, M. M., Truong-Hong, L., Samali, B. "A Decade of Modern Bridge Monitoring Using Terrestrial Laser Scanning: Review and Future Directions", Remote Sensing, 12(22), 3796, 2020. https://doi.org/10.3390/rs12223796

[3] Telling, J., Lyda, A., Hartzell, P., Glennie, C. "Review of Earth science research using terrestrial laser scanning", Earth-Science Reviews, 169, pp. 35–68, 2017. https://doi.org/10.1016/j.earscirev.2017.04.007

[4] Wujanz, D., Burger, M., Mettenleiter, M., Neitzel, F. "An intensity-based stochastic model for terrestrial laser scanners", ISPRS Journal of Photogrammetry and Remote Sensing, 125, pp. 146–155, 2017. https://doi.org/10.1016/j.isprsjprs.2016.12.006

[5] Truong-Hong, L., Laefer, D. F. "Application of terrestrial laser scanner in bridge inspection: review and an opportunity", In: 37th IABSE Symposium: Engineering for Progress, Nature and People, Madrid, Spain, 2014. Available at: http://hdl.handle.net/10197/7494

[6] Aryan, A., Bosché, F., Tang, P. "Planning for terrestrial laser scanning in construction: A review", Automation in Construction, 125, 103551, 2021. https://doi.org/10.1016/j.autcon.2021.103551

[7] Barneveld, R. J., Seeger, M., Maalen-Johansen, I. "Assessment of terrestrial laser scanning technology for obtaining high-resolution DEMs of soils", Earth Surface Processes and Landforms, 38(1), pp. 90–94, 2013. https://doi.org/10.1002/esp.3344

[8] Griebel, A., Bennett, L. T., Culvenor, D. S., Newnham, G. J., Arndt, S. K. "Reliability and limitations of a novel terrestrial laser scanner for daily monitoring of forest canopy dynamics", Remote Sensing of Environment, 166, pp. 205–213, 2015. https://doi.org/10.1016/j.rse.2015.06.014

[9] Mukupa, W., Roberts, G. W., Hancock, C. M., Al-Manasir, K. "A review of the use of terrestrial laser scanning application for change detection and deformation monitoring of structures", Survey Review, 49(353), pp. 99–116, 2017. https://doi.org/10.1080/00396265.2015.1133039

[10] Lovas, T., Barsi, Á., Detrekoi, A., Dunai, L., Csak, Z., Polgar, A., Berényi, A., Kibédy, Z., Szocs, K. "Terrestrial laser scanning in deformation measurements of structures", International Archives of Photogrammetry and Remote Sensing, 37(B5), pp. 527–531, 2008.

[11] Kasperski, J., Delacourt, C., Allemand, P., Potherat, P., Jaud, M., Varrel, E. "Application of a terrestrial laser scanner (TLS) to the study of the Séchilienne Landslide (Isère, France)", Remote Sensing, 2(12), pp. 2785–2802, 2010. https://doi.org/10.3390/rs122785

[12] Soudarissanane, S., Lindenbergh, R., Menenti, M., Teunissen, P. "Scanning geometry: Influencing factor on the quality of terrestrial laser scanning points", ISPRS journal of photogrammetry and remote sensing, 66(4), pp. 389–399, 2011. https://doi.org/10.1016/j.isprsjprs.2011.01.005

[13] Fischler, M. A., Bolles, R. C. "Random sample consensus: a paradigm for model fitting with applications to image analysis and automated cartography", Communications of the ACM, 24(6), pp. 381–395, 1981. https://doi.org/10.1145/358669.358692

[14] Matas, J., Chum, O. "Randomized RANSAC with sequential probability ratio test", In: Tenth IEEE International Conference on Computer Vision (ICCV'05) Volume 1, Beijing, China, pp. 1727–1732. ISBN 0-7695-2334-X https://doi.org/10.1109/ICCV.2005.198

[15] Raguram, R., Frahm, J.-M., Pollefeys, M. "A comparative analysis of RANSAC techniques leading to adaptive real-time random sample consensus", In: Computer Vision–ECCV 2008: 10th European Conference on Computer Vision, Marseille, France,, 2008, pp. 500–513. ISBN 978-3-540-88688-4 https://doi.org/10.1007/978-3-540-88688-4_37

[16] Urbančič, T., Vrečko, A., Kregar, K. "The Reliability of Ransac Method when Estimating the Parameters of Geometric Object", Geodetski Vestnik, 60(1), pp. 69–97, 2016.
https://doi.org/10.15292/geodetski-vestnik.2016.01.69-97

[17] Barnea, S., Filin, S. "Registration of terrestrial laser scans via image based features", International Archives of Photogrammetry, Remote Sensing and Spatial Information Sciences, 36(Part 3/W52), pp. 32–37, 2007.

[18] Capel, D. P. "An Effective Bail-out Test for RANSAC Consensus Scoring", In: British Machine Vision Conference, Oxford, UK, 2005, 78. ISBN 1-901725-29-4
https://doi.org/10.5244/C.19.78

[19] Huang, T., Zhang, D., Li, G., Jiang, M. "Registration method for terrestrial LiDAR point clouds using geometric features", Optical Engineering, 51(2), 021114, 2012.
https://doi.org/10.1117/1.OE.51.2.021114

[20] Li, Y., Ma, H., Wu, J. "Planar segmentation and topological reconstruction for urban buildings with lidar point clouds", In: International Symposium on Lidar and Radar Mapping 2011: Technologies and Applications, 2011, 828615.
https://doi.org/10.1117/12.912838

[21] Kim, T., Im, Y.-J. "Automatic satellite image registration by combination of matching and random sample consensus", IEEE Transactions on Geoscience and Remote Sensing, 41(5), pp. 1111–1117, 2003.
https://doi.org/10.1109/TGRS.2003.811994

[22] Maier, J., Humenberger, M. "Movement detection based on dense optical flow for unmanned aerial vehicles", International Journal of Advanced Robotic Systems, 10(2), 146, 2013.
https://doi.org/10.5772/52764

[23] Urbancic, T., Kosmatin Fras, M., Stopar, B., Koler, B. "The Influence of the Input Parameters Selection on the Ransac Results", International Journal of Simulation Modelling (IJSIMM), 13(2), pp. 159–170, 2014.
https://doi.org/10.2507/IJSIMM13(2)3.258

[24] Kim, D., Kwak, Y., Sohn, H. "Accelerated cable-stayed bridge construction using terrestrial laser scanning", Automation in Construction, 117, 103269, 2020.
https://doi.org/10.1016/j.autcon.2020.103269

[25] Schnabel, R., Wahl, R., Klein, R. "Efficient RANSAC for Point-Cloud Shape Detection", Computer Graphics Forum, 26(2), pp. 214–226, 2007.
https://doi.org/10.1111/j.1467-8659.2007.01016.x

[26] Gábor, P. "A Robinson híd" (The Robinson Bridge), Mérnök Újság, 29(1–2), pp. 26–27, 2022. (in Hungarian)